# $P$-wave coupled-channel scattering of $B_s\pi$, $B_s^*\pi$, $B\overline{K}$, $B^*\overline{K}$ and the puzzling $X(5568)$

Xian-Wei Kang* and J. A. Oller†
*Departamento de Física, Universidad de Murcia, E-30071 Murcia, Spain*

The D0 Collaboration has recently reported a narrow peak structure in the $B_s^0\pi^\pm$ invariant-mass spectrum, that is called $X(5568)$. Its proposed quantum numbers $J^P = 0^+/1^+$ are not determined unambiguously, and we show that one can fit the data assuming $J^P = 1^-$ with the same mass and width for the resonance signal. The corresponding isovector $P$-wave coupled-channel scattering involving the states $B_s\pi$, $B_s^*\pi$, $B\overline{K}$ and $B^*\overline{K}$ is studied employing leading-order Heavy Meson Chiral Perturbation Theory, which is then unitarized making use of standard techniques from Unitary Chiral Perturbation Theory. The subtraction constants that appear in the unitarization process are determined by a $u$-channel crossing symmetry constraint or by naturalness arguments, being the numerical values obtained in both cases quite closed, and no further freedom is left in the model. A crucial point is that if the $X(5568)$ is $1^-$ and decaying into $B_s^0\pi^\pm$ then it should appear as a pole in the $T$-matrix elements. It finally turns out that no $X(5568)$ pole is found that can be qualified as dynamically generated from the isovector $P$-wave coupled-channel dynamics. This result disfavors the interpretation of the $X(5568)$ within a "molecular" picture.

arXiv:1606.06665v1 [hep-ph] 21 Jun 2016

## I. INTRODUCTION

Recently, the D0 Collaboration has reported a narrow peak in the $B_s^0\pi^\pm$ mass spectrum, denoted as $X(5568)$, based on their 104 fb$^{-1}$ data of $p\bar{p}$ collision at $\sqrt{s} = 1.96$ TeV accumulated at the Fermilab Tevatron collider [1]. The resulting mass and width of this peak were determined as

$$m_X = 5567.8 \pm 2.9^{+0.9}_{-1.9}\,\text{MeV},$$
$$\Gamma_X = 21.9 \pm 6.4^{+5.0}_{-2.5}\,\text{MeV}, \quad (1)$$

respectively, and the spin-parity assignment $J^P = 0^+$ was used in the data analysis (with $1^+$ also discussed). In fact, the quantum numbers $J^P$ have not been well determined yet. The statistical significance was found to be $5.1\sigma$, including look-elsewhere effect and systematic uncertainties [1]. The decay of $X(5568)$ to $B_s^0\pi^\pm$ suggests that it has four valence quarks with different flavors: $su\bar{b}\bar{d}$ or $sd\bar{b}\bar{u}$. If finally the existence of the $X(5568)$ is confirmed, this will be the first observation of a resonance with all these quark flavors. This new finding has triggered the interest of theorists, and many interpretations have been proposed. Particularly, motivated by the aforementioned four quark components, one has models for tetraquark states [2–5], which typically show that their outcome is compatible with the experimental mass. Through a comparison between the molecular assignment and the diquark-antidiquark scenario within QCD sum rules, the tetraquark state is advocated in Ref. [6]. Although a four-quark ($[su][\bar{b}\bar{d}]$) state with $J^P = 0^+$ was found about 150 MeV higher than the $X(5568)$ using the diquark-antidiquark interaction in Ref. [2], the authors also claimed that the state is still likely to be identified as the $X(5568)$ once systematic errors in the model are considered. This state has also been analyzed within the quark model to further investigate the tetraquark components [7, 8]. In the former reference the calculated mass for $X(5568)$ is rather close to the experimental one, but the author also asks in the paper for a more elaborated model for the $sud\bar{b}$ system. The subsequent calculation in the relativized quark model [8] finds that the masses of $sq\bar{b}\bar{q}$ tetraquark states are much higher than the one of $X(5568)$, and thus the interpretation as a diquark-antidiquark state is disfavored. Later the dispute becomes more severe as LHCb fails to confirm such peak [9] using its 3 fb$^{-1}$ $pp$ collision data at $\sqrt{s} = 7$ and 8 TeV. In fact, several theoretical investigations e.g. Refs. [10, 11] point out that none of the models, including the threshold and cusp effects, molecular and tetraquark ones, give a satisfactory description of the $X(5568)$.

Already Ref. [10] discussed the possibility of the $X(5568)$ being generated from the $S$-wave coupled-channel transition of $B_s\pi \to B\overline{K}$, and performed a corresponding calculation within the nonrelativistic quark model. The authors concluded that this scenario is unlikely. This idea has been also implemented in the work of Ref. [12], where the $S$-wave potential between $B_s\pi$ and $B\overline{K}$ was calculated in the leading-order Heavy Meson Chiral Perturbation Theory (HMChPT), and then unitarized with the method of Ref. [13]. The free parameter, a subtraction constant or a three-momentum cutoff, is fitted to the experimental data on the $B_s^0\pi^\pm$ invariant-mass spectrum. It turns out that an unnaturally large cutoff, much larger than 1 GeV, is unavoidably needed to reproduce the mass of the resonance (with the resulting width in agreement with experiment). In this sense, the $X(5568)$ is hard to be assigned as a dynamically generated resonance by the $S$-wave $B_s\pi \to B\overline{K}$ scattering, disfavoring the molecular interpretation.

In fact, the quantum numbers $J^P$ for the resonance have not been determined unambiguously yet. The assignments $0^+$ ($X(5568) \to B_s^0\pi^\pm$) or $1^+$ ($X(5568) \to B_s^*\pi^\pm$ followed by $B_s^* \to B_s^0\gamma$) from Ref. [1] are purely based on fitting the resonance signal in the $B_s^0\pi^\pm$ event

* xianwei.kang@um.es
† oller@um.es

distribution with an $S$-wave Breit-Wigner (BW) function. We have also performed a purely phenomenological fit to the data of Ref. [1] in terms of a $P$-wave BW parameterization of the signal function with the same mass and width as in Eq. (1), and show that a reproduction nearly as good as the one assuming an $S$-wave BW results. In other terms, the current data is not capable of unambiguously pinning down the quantum numbers (and in particular the intrinsic parity) of the $X(5568)$. Another point that we want to stress here is that the mass threshold of $B_s^*\pi^+$ is below the pole position of $X(5568)$ only by around 10 MeV, closer indeed to the $X(5568)$ mass than the $B_s^0\pi^+$ threshold. Thus, from a "molecular" perspective for the generation of the $X(5568)$ it is suggestive to look for a coupled-channel-scattering scenario involving simultaneously $B_s\pi$ and $B_s^*\pi$. However, in order to conserve angular momentum and parity it is necessary at least a $P$-wave to couple both channels. It is typically considered that the $P$-wave scattering between $B_s\pi$ and $B_s^*\pi$ is small in the $X(5568)$ region because their three-momenta are small. However, the off-diagonal transitions involving the heavier $B\overline{K}$ and $B^*\overline{K}$ states have much larger *unphysical* three-momenta, determined by analytical continuation. This motivates our current study in coupled channels within HMChPT to study the isovector $P$-wave scattering between the channels $B_s\pi$, $B_s^*\pi$, $B\overline{K}$ and $B^*\overline{K}$. We also discuss that the subtraction constant per channel appearing in the unitarization process can be pinned down reliablly by imposing an $u$-channel crossing symmetry constraint, similarly as done in Refs. [14, 15]. The numerical values obtained in this way are also quite closed to the natural values that stem from a three-momentum cut-off around 1 GeV [16]. We conclude from our research that an explanation of the $X(5568)$ as dynamically generated resonance in $P$-wave scattering is not plausible.

This work is organized as follows. In Sec. II, we discuss the reproduction of the D0 data employing a $P$-wave BW parameterization for the signal function. Next we move to HMChPT in order to calculate the leading-order tree-level amplitudes projected in $P$-wave (Sec. III) and then its unitarization and following results are discussed in Sec. IV. At last, we conclude in Sec. V.

## II. INTERPRETATION OF D0 DATA WITH $B_s^0\pi^\pm$ IN $P$ WAVE

The $B_s^*\pi$ mass threshold is very close to the pole position of the $X(5568)$, as mentioned in the Introduction. The coupling of $B_s^*\pi$ to $B_s^0\pi$ requires at least a $P$-wave, because $S$-wave is not allowed due to angular momentum and parity conservation. These observations encourage us to reexamine the interpretation of the experimental data with $B_s^0\pi^\pm$ in $P$ wave and not in $S$ wave, as originally performed by the D0 Collaboration [1]. In this form the vector and pseudoscalar heavy mesons could scatter between each other within $P$-wave coupled-channel scattering (as analyzed in detail below in Sec. III and IV).

Before proceeding to the $P$-wave case, we review the formalism used by the D0 Collaboration [1] in fitting the invariant mass distribution of $B_s^0\pi^\pm$ assuming $S$-wave. The original full data contains both the background and the resonance signal. The extraction of the latter was done by fitting data without and with the "cone cut", as introduced in Ref. [1] in order to enhance the resonance signal. Both background components, that result with or without this cut, can be well parameterized as [17]

$$F_{\rm bgr}(m) = (c_0+c_2m^2+c_3m^3+c_4m^4)\exp(c_5+c_6m+c_7m^2)\,, \tag{2}$$

where $m \equiv m(B_s^0\pi^\pm)$ is the invariant mass of $B_s^0\pi^\pm$ (we use this shorthand notation in the following, if not otherwise stated). This parameterization reproduces perfectly well the background in all cases [1, 17].

A BW parameterization for a resonance of mass $M_X$ and width $\Gamma_X$ near the two-body threshold with orbital angular momentum $L$ can be written as

$$BW_L(m) \propto \frac{M_X^2\Gamma_X(m)}{(M_X-m)^2+M^2\Gamma_X^2(m)}\,. \tag{3}$$

This is written in terms of the mass-dependent width, which reads

$$\Gamma(m) = \Gamma_X\left(\frac{k(m)}{k(M_X)}\right)^{2L+1}\,, \tag{4}$$

and $k(m)$ is the magnitude of the center-of-mass (CM) three-momentum of $B_s^0\pi^\pm$ with invariant mass $m$, see Eq. (22) below for an explicit expression. As a result, the $P$-wave BW parameterization corresponds to replacing the factor $k(m)/k(M_X)$ in Ref. [1] by $(k(m)/k(M_X))^3$; i.e., the threshold behavior for the transition amplitude is implemented, see also the review "Resonances" in PDG [18].

Analogously to Ref. [1] we first fit the full data with the function

$$F(m) = f_{\rm sig}\times BW_0(m) + f_{\rm bgr}\times F_{\rm bgr}(m)\,, \tag{5}$$

where the resonance signal is parameterized in terms of an $S$-wave BW times a normalization constant $f_{\rm sig}$. The background is given in terms of $F_{\rm bgr}(m)$, cf. Eq. (2), times the constant $f_{\rm bgr}$. Both $f_{\rm sig}$ and $f_{\rm bgr}$ are fitted to data, while $M_X$ and $\Gamma_X$ are fixed according to their experimental numbers in Eq. (1) obtained by the D0 Collaboration. The resulting curves are given by the dashed lines in Fig. 1 (the upper panel corresponds to the case with the "cone cut" and the bottom one without this cut) and closely reproduce data.

However, the parameterization of the signal function by an $S$- or $P$-wave BW cannot be really ascertained by the present experimental data [1]. This can be easily seen by directly replacing $BW_0(m)$ in Eq. (5) by $BW_1(m)$ (with the same mass and width) and refitting $f_{\rm sig}$ and $f_{\rm bgr}$. The change for these parameters is small, being around a 5% for the former and a 2% for the latter. The

result of this fit is shown by the solid lines in Fig. 1, which can hardly be distinguished from the dashed lines corresponding to the $S$-wave BW parameterization of the signal function. Because of the close proximity between the $S$- and $P$-wave BW fits and their good reproduction of data, we skip distinguishing between partial and total decay widths of the $X(5568)$ in Eq. (3). Notice that for a $1^-$ resonance the $B_s^*\pi^+$ channel is also open since $M_X$ is slightly larger (around 10 MeV) than its threshold.

Thus, one cannot exclude a $P$-wave scenario for the invariant mass distribution of $B_s^0\pi^\pm$ from the decay of the $X(5568)$ resonance, with the present data determined by the D0 Collaboration [1]. As remarked in Ref. [19], an angular distribution analysis should be performed in order to further constraint the quantum numbers of the $X(5568)$ and check any model on this resonance. In the rest of this work we are going to consider the assignment $J^P = 1^-$ for the $X(5568)$, a vector state, and explore its possible dynamical generation from coupled-channel scattering of $B_s^0\pi^+$, $B_s^*\pi^+$, $B^+\overline{K}^0$ and $B^{*+}\overline{K}^0$.

## III. COUPLED-CHANNEL POTENTIAL

Assuming that the $X(5568)$ is an $1^-$ state, $B_s^0\pi^+$ scattering occurs in $P$-wave, in which case, the transition between $B_s^0\pi^+$ (1), $B_s^*\pi^+$ (2), $B^+\overline{K}^0$ (3) and $B^{*+}\overline{K}^0$ (4) are allowed. In this list the channels have been labeled in increasing order of their mass thresholds: 5506.36 MeV, 5554.97 MeV, 5772.29 MeV, 5818.10 MeV, respectively. Such a coupled-channel system can be treated in Heavy Meson Chiral Perturbation Theory (HMChPT) [20–22]. Here, we closely follow Wise's convention in Ref. [20]. The interactions of the heavy mesons ($B^{(*)}$ or $B_s^{(*)}$) and the pseudo-Goldstone bosons ($\pi$, $K$, $\eta$) are described at leading order in HMChPT by the Lagrangian

$$\begin{aligned}\mathscr{L} &= \frac{i}{2}\mathrm{Tr}\,\overline{H}_a H_b v^\mu(\xi^\dagger\partial_\mu\xi + \xi\partial_\mu\xi^\dagger)_{ba} \\ &\quad + \frac{ig}{2}\mathrm{Tr}\,\overline{H}_a H_b\gamma^\mu\gamma_5(\xi^\dagger\partial_\mu\xi - \xi\partial_\mu\xi^\dagger)_{ba}\,, \end{aligned} \tag{6}$$

with the $SU(3)$ subscripts $a$ and $b$ running from 1 to 3. The quantity $v$ is the four-velocity of the heavy meson, whose four-momentum can be parameterized as

$$p = m\,v\,+\,q, \tag{7}$$

with $q$ a small residual four-momentum. The $H_a$ fields are defined as

$$\begin{aligned} H_a &= \frac{1+\not{v}}{2}\left(P^*_{a\mu}\gamma^\mu - P_a\gamma_5\right)\,, \\ \overline{H}_a &= \gamma^0 H_a^\dagger\gamma^0\,, \end{aligned} \tag{8}$$

with the heavy meson fields containing the heavy $b$ quark:

$$\begin{aligned} (P_1, P_2, P_3) &= (B^-, \overline{B}^0, \overline{B}_s^0)\,, \\ (P_1^*, P_2^*, P_3^*) &= (B^{*-}, \overline{B}^{*0}, \overline{B}_s^*)\,, \end{aligned} \tag{9}$$

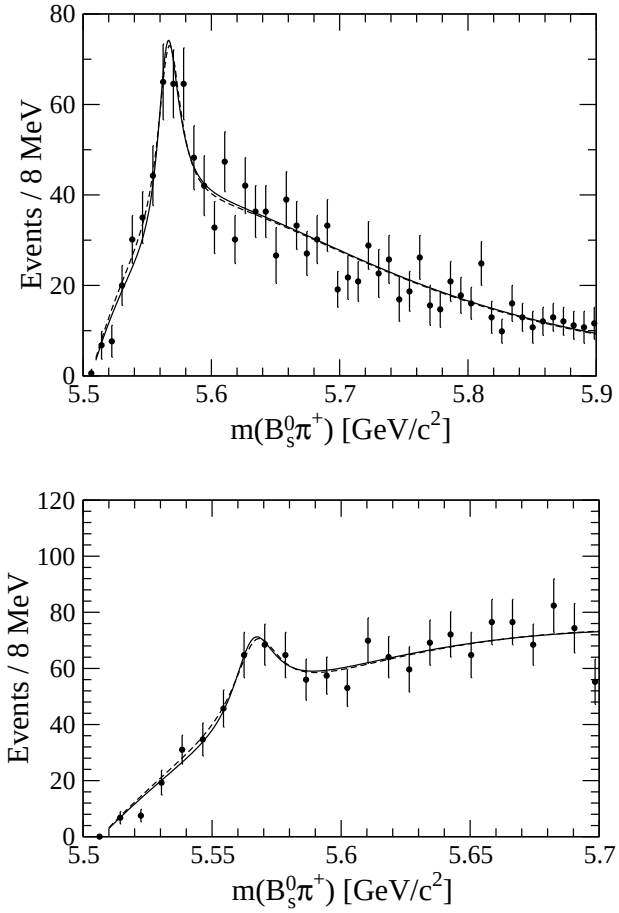


FIG. 1. Invariant mass distribution for $B_s^0\pi^\pm$ with the data taken from Ref. [1]. The upper (lower) panel corresponds to the case with (without) the "cone cut" [1]. The solid (dashed) lines represent our results with the mass and width of the resonance given by Eq. (1) for the $P$-($S$-)wave BW parameterizations of the signal function.

and $P$ ($P^*$) denotes a heavy pseudoscalar (vector) meson. The symbol Tr in Eq. (6) indicates the trace taken over the Dirac matrices. The light pseudoscalar mesons are contained in the $3\times 3$ matrix $\xi$, defined as

$$\xi = \exp\left(\frac{i\phi}{\sqrt{2}f_\pi}\right)\,, \tag{10}$$

where

$$f_\pi \approx 92.4\ \mathrm{MeV} \tag{11}$$

is the (leading-order) pion decay constant and

$$\phi = \begin{pmatrix} \frac{\pi^0}{\sqrt{2}} + \frac{\eta}{\sqrt{6}} & \pi^+ & K^+ \\ \pi^- & -\frac{\pi^0}{\sqrt{2}} + \frac{\eta}{\sqrt{6}} & K^0 \\ K^- & \overline{K}^0 & -\sqrt{\frac{2}{3}}\eta \end{pmatrix}\,.$$

In the original reference [20], another convention on the pion decay constant, $f = \sqrt{2}f_\pi \approx 130$ MeV, was used. Note also that $v_\mu P^{*\mu} = 0$ due to the Lorenz condition.

Explicitly, from the Lagrangian in Eq. (6) we obtain the following terms relevant for $B_s^0\pi^+$ plus coupled-channel scattering

$$\begin{aligned}\mathscr{L} = &-\frac{\sqrt{2}g}{f_\pi}\left(P_a^{*\dagger\alpha}\,P_b + P_a^\dagger P_b^{*\alpha}\right)(\partial_\alpha\phi)_{ba}\\ &-\frac{i\sqrt{2}g}{f_\pi}\,\epsilon^{\mu\nu\sigma\alpha}\,P_{a\mu}^{*\dagger}\,P_{b\nu}^{*}\,v_\sigma\,(\partial_\alpha\phi)_{ba}\\ &+\frac{i}{2f_\pi^2}\,P_{a\mu}^{*\dagger}\,P_b^{*\mu}\,v^\alpha\,(\phi\,\partial_\alpha\phi - \partial_\alpha\phi\,\phi)_{ba}\\ &-\frac{i}{2f_\pi^2}\,P_a^\dagger\,P_b\,v^\alpha\,(\phi\,\partial_\alpha\phi - \partial_\alpha\phi\,\phi)_{ba} + \dots \quad (12)\end{aligned}$$

from which the interaction vertices can be read off easily. The ellipsis in the previous equation indicates terms that also contribute to $\mathcal{L}$ but are not of interest here. Each term in Eq. (12) from the the first to the fourth line gives rise to a vertex involving $P^*P\phi$, $P^*P^*\phi$, $P^*P^*\phi\phi$, $PP\phi\phi$, respectively. For our present purposes each $P$ ($P^*$) denotes a heavy pseudoscalar (vector) belonging to the $B$ ($B^*$) family, and every $\phi$ contributes with a pseudo-Goldstone boson ($\pi$, $K$, $\eta$). The fact that $B^*$ cannot decay to $B\pi$ ($m_{B^*} < m_B + m_\pi$) complicates the determination of $g$ by experiment in the $B$ sector. However, it has been studied extensively within lattice QCD. The most recent determination can be found in Ref. [23], where $g_{B^*B\pi} = 0.56 \pm 0.08$ is reported, where we have added the statistical and systematic errors in quadrature. Previous results from lattice QCD calculations are also organized and compared in this reference, and they agree within uncertainties. Under the heavy quark flavor symmetry, one has also that $g = g_{D^*D\pi}$, which can be rather well determined from the experimental decay width of $D^{*+} \to D^0\pi^+$. The result is $g = g_{D^*D\pi} = 0.58 \pm 0.07$, with the error obtained from the uncertainty of the $D^{*+}$ width [24]. This is in a perfect agreement with the lattice QCD results. In the numerical calculations we use the value determined from phenomenology, as also done in Ref. [24].

Based on the above Lagrangian, we can list out and calculate the Feynman diagrams at the leading order, which are drawn in Fig. 2. Here the heavy vector (pseudoscalar) mesons are indicated by double (single) solid lines and the light pseudoscalar mesons ($\pi^+$ and $\overline{K}^0$) by dashed lines. From the first to fourth line, they contribute to $V_{13} \equiv V_{B_s^0\pi^+\to B^+\overline{K}^0}$, $V_{14} \equiv V_{B_s^0\pi^+\to B^{*+}\overline{K}^0}$ $V_{23} \equiv V_{B_s^*\pi^+\to B^+\overline{K}^0}$ and $V_{24} \equiv V_{B_s^*\pi^+\to B^{*+}\overline{K}^0}$, respectively. In $V_{13}$ and $V_{24}$, there are two diagrams, labeled by the subscripts 1 and 2, from left to right. All other contributions vanish in the $4\times 4$ potential matrix and, in particular, there are neither $s$-channel nor $t$-channel exchange diagrams at leading order. After the calculation, we obtain the potentials in the rest frame of heavy particles (i.e. $v = (1,0,0,0)$):

$$V_{13,1} = \frac{\sqrt{m_B m_{B_s}}}{2f_\pi^2}(E_\pi + E_K)\,,$$

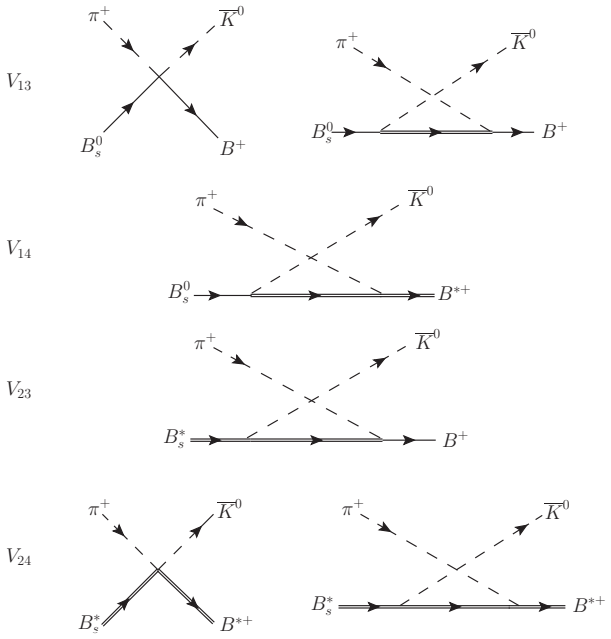


FIG. 2. The leading-order Feynman diagrams in HMChPT contributing to the $4\times 4$ potential matrix $V_{ij}$. The double (single) lines represent heavy vectors (pseudoscalars) and the dashed lines denote the light pseudoscalars $\pi^+$ or $\overline{K}^0$.

$$\begin{aligned}V_{13,2} &= -\frac{2g^2\sqrt{m_{B_s}m_B}}{f_\pi^2}\frac{m_B}{u-m_{B^*}^2}\mathbf{p}_\pi\cdot\mathbf{p}_K\,,\\ V_{14} &= \frac{2ig^2\sqrt{m_{B_s}m_{B^*}}}{f_\pi^2}\frac{m_{B^*}}{u-m_{B^*}^2}\boldsymbol{\varepsilon}'^*\cdot(\mathbf{p}_K\times\mathbf{p}_\pi)\,,\\ V_{23} &= \frac{2ig^2\sqrt{m_{B_s^*}m_B}}{f_\pi^2}\frac{m_B}{u-m_{B^*}^2}\boldsymbol{\varepsilon}\cdot(\mathbf{p}_K\times\mathbf{p}_\pi)\,,\\ V_{24,1} &= \frac{\sqrt{m_{B_s^*}m_{B^*}}}{2f_\pi^2}(E_\pi+E_K)\boldsymbol{\varepsilon}\cdot\boldsymbol{\varepsilon}'^*\,,\\ V_{24,2} &= \frac{2g^2\sqrt{m_{B_s^*}m_{B^*}}}{f_\pi^2}\frac{m_{B^*}}{u-m_{B^*}^2}\\ &\quad\times(\boldsymbol{\varepsilon}\cdot\boldsymbol{\varepsilon}'^*\,\mathbf{p}_K\cdot\mathbf{p}_\pi - \boldsymbol{\varepsilon}\cdot\mathbf{p}_\pi\,\boldsymbol{\varepsilon}'^*\cdot\mathbf{p}_K)\,. \quad (13)\end{aligned}$$

In this equation the symbols $E_K$ and $E_\pi$ refer to the kaon and pion energy, in order, and should be calculated accordingly to the scattering channels involved. E.g. $V_{13}$ corresponds to $B_s^0\pi^+ \to B^+\overline{K}$ and then in the heavy-meson limit $E_\pi = \sqrt{s} - m_{B_s^0}$ and $E_K = \sqrt{s} - m_{B^+}$, with $s$ the standard Mandelstam variable. In terms of $E_K$ and $E_\pi$, the modulus of the kaon and pion three-momenta are $|\mathbf{p}_\pi| = \sqrt{E_\pi^2 - m_\pi^2}$ and $|\mathbf{p}_K| = \sqrt{E_K^2 - m_K^2}$. The standard Mandelstam variable $u$ in the heavy-meson limit simplifies to $m_{B'}^2 - 2m_{B'}E_\pi$, with $m_{B'}$ the mass of the final heavy meson.[1] In this form the propagators in

[1] In the study of $B\to\pi\pi l\bar{\nu}_l$ by Ref. [24], the full relativistic prop-

Eq. (13), $m_{B'}/(u-m_{B^*}^2)$, tend to the standard form in HMChPT. E.g. for $V_{13}$

$$\frac{m_B}{u-m_{B^*}^2} \to -\frac{1}{2(\Delta+E_\pi)}\,, \tag{14}$$

where $\Delta$ is the mass difference $m_{B^*}-m_B$, and similar results apply to the other transitions between channels. Note also that factors of $\sqrt{m_P}$ and $\sqrt{m_{P^*}}$ have been included in the definition of $P$ and $P^*$ fields.

The symbols $\boldsymbol{\varepsilon}$ and $\boldsymbol{\varepsilon}'$ in Eq. (13) represent the polarization vectors for the incoming and outgoing heavy vector mesons in spherical basis, respectively. As a result of the large masses of the $B$ and $B^*$ we can take the polarization vectors in the rest frame of the heavy vectors. In the Cartesian basis they can be written as

$$\vec{\epsilon}_1=\begin{pmatrix}1\\0\\0\end{pmatrix}\,,\quad \vec{\epsilon}_2=\begin{pmatrix}0\\1\\0\end{pmatrix}\,,\quad \vec{\epsilon}_3=\begin{pmatrix}0\\0\\1\end{pmatrix}\,. \tag{15}$$

In the spherical basis they are given by

$$\boldsymbol{\varepsilon}(\pm1)=\mp\frac{1}{\sqrt{2}}(\vec{\epsilon}_1\pm i\vec{\epsilon}_2)\,,\quad \boldsymbol{\varepsilon}(0)=\vec{\epsilon}_3, \tag{16}$$

and take the form

$$\boldsymbol{\varepsilon}(\pm1)=\mp\frac{1}{\sqrt{2}}\begin{pmatrix}1\\ \pm i\\ 0\end{pmatrix}\,,\quad \boldsymbol{\varepsilon}_3=\begin{pmatrix}0\\0\\1\end{pmatrix}\,. \tag{17}$$

It follows then that both $V_{13,1}$ and $V_{24,1}$ do not involve any angular dependence, and thus they only contribute to $S$-wave. The $\sqrt{m_1 m_2}$ factors appearing in Eq. (13) can be safely replaced by just $m_{B_s^0}$, since the biggest difference can be $(m_{B_s^*}-m_{B^+})/m_{B_s^0}\sim m_\pi/m_{B_s^0}<3\%$. However, the mass splittings play a more important role in the unitarity two-point loop functions due to the proximity of the associated branch-point singularity for the first and second channels to the $X(5568)$ nominal mass, i.e., the most important heavy-quark symmetry breaking corrections arise from the unitarization. Such strategy has also been widely adopted in many instances of coupled-channel studies, see e.g. the recent $\pi\Sigma_c$ scattering study in Ref. [25]. In principle, one should work in the CM, however, we have checked that in the kinematic region that we consider, $5.5\,\text{GeV}<\sqrt{s}<5.7\,\text{GeV}$, differences are only about a few percent compared with Eq. (13), which is worked out in rest frames of the heavy mesons. For instance, the term $\sqrt{m_{B^+}m_{B_s^0}}(E_K+E_\pi)$ in $V_{13,1}$ comes from $\sqrt{m_{B^+}m_{B_s^0}}v\cdot(p_K+p_\pi)$, a term that is replaced by $(p_{B_s^0}+p_{B^+})\cdot(p_K+p_\pi)/2$ using the covariant Lagrangian [21] (the one used in Ref. [12]). It turns out that these two forms differ only by a few percent. Specially, the ratio of the covariant one (that could be the most precise form) to the form used here in the region around the mass of $X(5568)$ is inside the range [0.998, 1]. The lack of relevance of these corrections is due to the small velocity involved in the Lorentz transformations from the heavy-meson rest frames to the CM one.

We proceed now to the $P$-wave projection of the tree-level amplitudes in Eq. (13). To that end, there are several ways to perform the partial wave decomposition. One consists of working first in the helicity basis [26], and then transforming into partial wave $lSJ$ basis, see e.g., [27] for the case of nucleon-nucleon ($NN$) scattering. Another one employs the tensor formalism [28], see e.g., [29] again for $NN$ scattering. We follow here the formalism developed in Ref. [30], which establishes that the partial-wave amplitude for the scattering $1+2\to1'+2'$ can be written generally as

$$\begin{aligned}V_{JI}(l'\,S',l\,S)=&\frac{Y_l^0(\hat{z})}{2J+1}\sum\langle s_1'\sigma_1' s_2'\sigma_2'|S's_3'\rangle\langle s_1\sigma_1 s_2\sigma_2|Ss_3\rangle\\ &\times\langle l0Ss_3|Js_3\rangle\langle l'm'S's_3'|Js_3\rangle\langle\tau_1'\alpha_1'\tau_2'\alpha_2'|Ii_3\rangle\langle\tau_1\alpha_1\tau_2\alpha_2|Ii_3\rangle\\ &\times\int d\Omega\, V(\vec{p}\,',\sigma_1'\alpha_1'\sigma_2'\alpha_2';\,p\hat{z},\sigma_1\alpha_1\sigma_2\alpha_2)Y_{l'}^{m'}(\theta,\phi)^*,\end{aligned} \tag{18}$$

where the repeated indices for the third components of spin-like quantities (including isospin) are summed. On the left hand side of the previous equation $(l,\,S)\,[(l',\,S')]$ is the orbital angular momentum and total spin in the initial [final] state, and $I$ and $J$ are the total isospin and angular momentum, in order, which are conserved in the scattering process; in our present case $I=J=1$. On the right hand side of Eq. (18), we have denoted the Clebsch-Gordan coefficients (CGC) by $\langle j_1m_1j_2m_2|jm\rangle$, where $m_1$, $m_2$ and $m=m_1+m_2$ are the third components of the angular momenta $j_1,j_2,j$, respectively. One can easily identify in Eq. (18) that the product of the two CGCs in the first line corresponds to the composition of the final/initial spins to the total one. Analogously, the product of the first two CGCs in the second line is for the composition of the orbital angular momentum and total spin to give the total angular momentum, and the last two CGCs in the same line proceed similarly for the isospin. Within the integration the scattering amplitude, here referred by $V$, is calculated in the well-defined three-momentum basis with the corresponding isospin and spin indices for each particle. Besides, $Y_l^m(\theta,\phi)$ is the standard spherical harmonics function, and fixing the $z$-axis along the initial three-momentum $\mathbf{p}$ the solid angle of the final three-momentum $\mathbf{p}'$ is parameterized by $(\theta,\phi)$. For our current case, the spin and isospin parts just contribute with a factor of one each. In case of the scattering involving pure spin-0 particles, Eq. (18) simplifies

agators are kept, rather than the leading term in the expansion of $1/m_P$ or $1/m_{P^*}$, as meant in Eq. (14), in order not to miss any analytic structure of the $B^*\pi\pi$ triangle graph in $\pi\pi$ rescattering. However, in our current situation, we are dealing with two-point unitarity loop functions and the form of the heavy meson propagator in Eq. (13) can be used without problem.

into the well-known form

$$T(s,\cos\theta)=\sum_l (2l+1)T_l(s)P_l(\cos\theta), \tag{19}$$

with $P_l(\cos\theta)$ denoting a Legendre polynomial.

The resulting $P$-wave projections of the amplitudes in Eq. (13) as follows from Eq. (18) are

$$\begin{aligned}
V_{13,\,l=l'=1} &= -\frac{2g^2 m_B\sqrt{m_{B_s}m_B}}{3f_\pi^2(u-m_{B^*}^2)}|\mathbf{p}_\pi||\mathbf{p}_K|\,,\\
V_{14,\,l=l'=1} &= -\frac{\sqrt{8}g^2 m_{B^*}\sqrt{m_{B_s}m_{B^*}}}{3f_\pi^2(u-m_{B^*}^2)}|\mathbf{p}_\pi||\mathbf{p}_K|\,,\\
V_{23,\,l=l'=1} &= -\frac{\sqrt{8}g^2 m_B\sqrt{m_{B_s^*}m_B}}{3f_\pi^2(u-m_{B^*}^2)}|\mathbf{p}_\pi||\mathbf{p}_K|\,,\\
V_{24,\,l=l'=1} &= \frac{2g^2 m_{B^*}\sqrt{m_{B_s^*}m_{B^*}}}{3f_\pi^2(u-m_{B^*}^2)}|\mathbf{p}_\pi||\mathbf{p}_K|.
\end{aligned} \tag{20}$$

## IV. RESULTS AND DISCUSSION

The potential calculated in Sec. III is the leading-order prediction in HMChPT. We want to take into account final state interactions by implementing the unitarization procedure of Ref. [13], where the potential is treated on shell and the Bethe-Salpeter equation can then be solved algebraically. This procedure can be also seen as a result of solving the $N/D$ method, firstly taking only into account the right-hand or unitarity cut and then including it perturbatively by matching with the chiral expansion order by order [16, 31, 32]. In the dimensional regularization scheme, the renormalized unitarity two-point loop function for channel $i$ (with masses $m_{1i},\ m_{2i}$) can be expressed as [33, 34]

$$\begin{aligned}
G_i(s) =& \frac{1}{(4\pi)^2}\left(\alpha_i(\mu)+\log\frac{m_{2i}^2}{\mu^2}-\varkappa_+\log\frac{\varkappa_+-1}{\varkappa_+}\right.\\
&\left.-\varkappa_-\log\frac{\varkappa_--1}{\varkappa_-}\right)\,,
\end{aligned} \tag{21}$$

where $\alpha_i(\mu)$ is a subtraction constant at the renormalization scale $\mu$ and

$$\begin{aligned}
\varkappa_\pm =& \frac{s+m_{1i}^2-m_{2i}^2}{2s}\pm\frac{k_i}{\sqrt{s}}\,,\\
k_i =& \frac{\sqrt{(s-(m_{1i}-m_{2i})^2)(s-(m_{1i}+m_{2i})^2)}}{2\sqrt{s}}\,,
\end{aligned} \tag{22}$$

The coupled-channel scattering $T$-matrix can be written as [13, 31][2]

$$T^{-1}(s)=V^{-1}(s)+G(s). \tag{23}$$

[2] Note the change of sign in the convention for $T(s)$ and $V(s)$ used here with respect to that in Refs. [13, 31].

In our current case, $V(s)$ and $T(s)$ are $4\times 4$ matrices incorporating the coupled-channel transitions. The potential matrix $V(s)$ has been elaborated in detail in Sec. III and we will use its $P$-wave projection, given in Eq. (20). The four-dimensional diagonal matrix $G(s)$ contains the two-point loop functions for all channels. If there is a pole at $s_X$, the determinant of the right hand of Eq. (23) should be zero at $s_X$. We denote by $\Delta(s)$ to this determinant, namely,

$$\Delta(s)=\det\left[V^{-1}(s)+G(s)\right]. \tag{24}$$

Since a resonance appears in the unphysical Riemann sheets, we need the analytic continuation of $G_i(s)$ from the physical (first) sheet (i.e., Eq. (21)) to the unphysical one associated to this channel. This analytical continuation is given by [13]

$$G_i^{II}(s)=G_i(s)+i\frac{k_i}{4\pi\sqrt{s}}, \tag{25}$$

where $k_i$ is calculated such that $\mathrm{Im}\,k_i>0$ as in the physical sheet. The experimentally reported mass of $X(5568)$ is around 5568 MeV, cf. Eq. (1), which stays between the mass thresholds of channels $B_s^*\pi^+$ (2) and $B^+\overline{K}^0$ (3), i.e., $m_{B_s'^0}+m_\pi<m_X<m_B+m_K$. Thus, we work in the unphysical Riemann sheets of channels (1) and (2), and in the physical sheets of channels (3) and (4), because the Laurent expansion around the resonance pole embraces the physical energy axis between channels (2) and (3). This Riemann sheet is named as (1,1,0,0), where the number 1 indicates that the analytical continuation to the unphysical sheet of the corresponding channel is applied. The $G$ matrix in the (1,1,0,0) Riemann sheet is

$$G(s)=\mathrm{diag}\left\{G_1^{II}(s),\,G_2^{II}(s),\,G_3(s),\,G_4(s)\right\} \tag{26}$$

Other sheets in this notation can be inferred easily (and indeed they have been also explored, particularly the closer (1,0,0,0) sheet).

We now elaborate about the subtraction constant in Eq. (21). The crossed $u$-channel $P$-wave scattering settles the constraint that after unitarizing the exchange of the $B^{*0}$ must give rise to a simple pole located at the same position as in the Born term, that is, at $u=m_{B^{*0}}^2$. The channels involved in the $s$-channel scattering becomes after $u$-crossing $B_s^0K^0$ (1), $B_s^*K^0$ (2), $B^+\pi^-$ (3) and $B^{*+}\pi^-$ (4). The $P$-wave projected leading-order HMChPT amplitudes in the $u$-channel look the same as those in Eq. (20). However, now $u$ does not vary between channels (in the same was as $s$ is the same for all channels in $s$-channel scattering), the three-momenta are calculated in terms of $u$ (not $s$) and one has to keep in mind the rearrangement of mesons in the new channels with zero strangeness. In the following, in order to avoid using the same symbols for both $s$- and $u$-channel scattering we place a tilde on top of the symbols for the latter case. The unitarization process is then performed making use of Eq. (23) and, in order that the

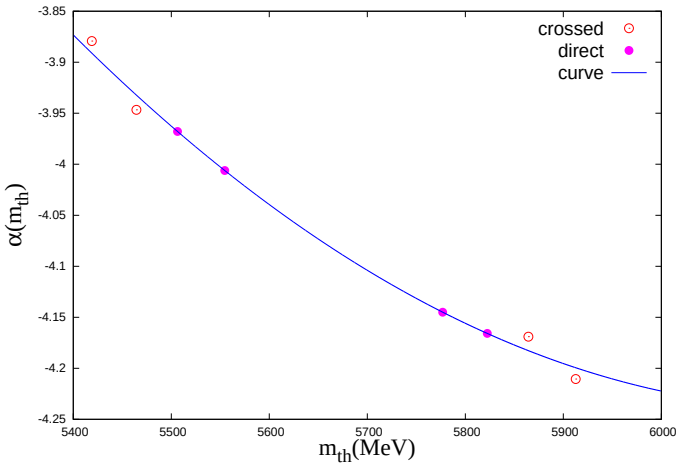


FIG. 3. Subtraction constants $\widetilde{\alpha}_i(M_\rho)$ and $\alpha_i(M_\rho)$ as a function of the threshold mass, given by the empty and filled circles, in order. The solid line is a parabola fit to the former ones, cf. Eq. (27).

resulting partial-wave amplitudes have a simple pole at $u = m^2_{B^{*0}}$, it is required that all the two-point unitarity wave functions vanish at that point. This is clear because then $\widetilde{T}(u) = [I + \widetilde{V}(u)\cdot\widetilde{G}(u)]^{-1}\cdot\widetilde{V}(u)$ (a rewriting of Eq. (23)) and the condition $\widetilde{G}(m^2_{B^*}) = 0$ imply that the matrix $[I + \widetilde{V}(u)\cdot\widetilde{G}(u)]^{-1}$ does not contain any pole at $u = m^2_{B^{*0}}$, so that both $\widetilde{T}(u)$ and $\widetilde{V}(u)$ have a simple pole there.[3] The subtraction constants for the $u$-channel states, indicated by $\widetilde{\alpha}_i$, can then be evaluated straightforwardly from the condition $\widetilde{G}(m^2_{B^{*0}}) = 0$, cf. Eq. (21), and the resulting values for $\mu = 770$ MeV $\simeq M_\rho$ are plotted by the empty circles in Fig. 3 as a function of the two-body threshold. These values are around $-4$ and we observe that they mainly follow a linear behavior with some small curvature. We then fit these points with the curve

$$\widetilde{\alpha}(m_{\rm th}) = a + b m_{\rm th} + c m^2_{\rm th} \ , \qquad (27)$$

which reproduces rather well the input points, as shown by the solid line in Fig. 3. Once this is set up we can reliably determine from Eq. (27) the value of the $s$-channel subtractions constants $\alpha_i(\mu)$ for our original problem on $s$-channel $P$-wave scattering. The values are shown in Fig. 3 by the filled circles. We then search for the zeros of $\Delta(s)$, cf. Eq. (24), in the complex plane of (1,1,0,0) and (1,0,0,0) sheets. The result of this search is that no pole is found there in the region of the $X(5568)$.

The values for the subtraction constants in Fig. 3 are indeed quite close to their natural values according to Ref. [16]. This reference exploits the fact that an apparent meaning for "natural" can be found in three-momentum cutoff regularization. Namely, the three-momentum cutoff $\Lambda$ should be around the chiral expansion scale, or more intuitively speaking, it should correspond to the scale in configuration space around the finite size of particles. Here the natural value for $\Lambda$ is about the $\rho$ mass or 1 GeV. By comparing Eq. (21) with the one in the cutoff regularization (Eq. (29) below), one finds [16]

$$\alpha_i(\mu_i) = -2\log\left(1 + \sqrt{1 + \frac{m^2_{2i}}{\mu_i^2}}\right) , \qquad (28)$$

where in the channel $i$, $m_{2i}$ is the heavier mass, e.g., for channel $B^0_s\pi^+$, $m_{21} = m_{B^0_s}$ and $m_{11} = m_{\pi^+}$. Powers of $k_i^2$ and $m_{1i}/m_{2i}$ have been neglected in obtaining Eq. (28). As with the values of the subtraction constants given by the filled points in Fig. 3, the search for zeros of $\Delta(s)$ using Eq. (28) is also fruitless.

A more radical strategy to try to reproduce the $X(5568)$ pole would be to treat the subtraction constants $\alpha_i$ as free parameters, so as to impose a pole at $\sqrt{s_X} \approx 5568 - i\,11$ MeV. Of course, in this form the $u$-channel crossed-exchange constraint $\widetilde{G}(m^2_{B^{*0}}) = 0$ is not satisfied. Using a unique subtraction constant shared by all the four loop functions, one can solve the equation $|\Delta(s_X)| = 0$ and four sets of *complex* solutions result then, which are not acceptable because they drive to violations of unitarity (on top of the mentioned one from crossing). When we fix two *real* subtraction constants around their values in Fig. 3 in a short region, one can determine the other two *real* subtraction constants by solving the equations $\mathrm{Re}\,\Delta(s_X) = 0$ and $\mathrm{Im}\,\Delta(s_X) = 0$. It turns out that no solutions in the natural-size range can be found; e.g., by fixing $\alpha_2 = -4$, $\alpha_4 = -4.15$, one gets $\alpha_1 = -1.8$, $\alpha_3 = -114.8$ or $\alpha_1 = 382.5$, $\alpha_3 = -1.2$. There are other regions in the parametric space $(\alpha_2, \alpha_4)$ that also drive to real $(\alpha_1, \alpha_3)$ parameters, but all of them are very far from the region of natural values for the $\alpha_i(\mu)$. Thus, there is no appropriate solution that can give rise to an $X(5568)$ dynamically generated from the interactions of $B_s\pi^+$ plus coupled-channels in $P$-wave scattering. Of course, as follows from the discussion, one could impose the $X(5568)$ pole but then it would correspond to a new elementary degree of freedom of unknown origin. That is, the generation of the pole could be reproduced but we could not deduce any explanation about its origin, as we are seeking.

Next, we take the functions $G_i(s)$ calculated with a common three-momentum cutoff, $\Lambda$, to further confirm the above findings and because it is also used in the study of Ref. [12] on $B_s\pi$ and $B\overline{K}$ $S$-wave scattering. The two-

[3] Another possible solution is to employ in the Born terms a bare mass for the particle exchanged that is dressed so as to end with the proper pole, see e.g. Ref. [35]. We have followed here the procedure of Refs. [14] and [15], which is the most suitable one when calculating higher orders in the chiral perturbative series. This is so because by using the physical mass in the Born terms one can avoid double-pole terms that otherwise would appear in the perturbative series, see also Ref. [36].

point unitarity loop function regularized with a three-momentum cutoff $\Lambda$ was calculated in Ref. [37]. It reads

$$G_i(s) = \frac{1}{16\pi^2}\left[-\frac{\delta}{2s}\log\frac{m_{1i}^2}{m_{2i}^2} + \frac{\nu_i}{2s}\left(\log\frac{s-\delta+\nu_i\lambda_1}{-s+\delta+\nu_i\lambda_1} + \log\frac{s+\delta+\nu_i\lambda_2}{-s-\delta+\nu_i\lambda_2}\right) + \frac{\delta}{s}\log\frac{1+\lambda_1}{1+\lambda_2} - \log[(1+\lambda_1)(1+\lambda_2)] + \log\frac{m_{1i}m_{2i}}{\Lambda_i^2}\right], \quad (29)$$

with

$$\nu_i = 2\sqrt{s}k_i\,, \quad \delta = m_{2i}^2 - m_{1i}^2\,, \quad \lambda_1 = \sqrt{1+\frac{m_{1i}^2}{\Lambda_i^2}}\,, \quad \lambda_2 = \sqrt{1+\frac{m_{2i}^2}{\Lambda_i^2}}\,. \quad (30)$$

and $k_i$ is given in Eq. (22). Both Eq. (21) and Eq. (29) are symmetric under the exchange of $m_{1i} \leftrightarrow m_{2i}$. The analytic continuation to the unphysical sheet is also given by Eq. (25). We have looked for poles of $1/\Delta(s_X)$ by varying $\Lambda$ (shared by all the four $G_i(s)$ in Eq.(29)), and find that this function changes smoothly in a rather large region of $\Lambda$ (a much wider region than the natural one around 1 GeV). Being inspired by the functional dependence of the estimation of the natural value for the subtraction constants on $m_{2i}$, cf. Eq. (28), we further assume that channels (1) and (2) share a cutoff $\Lambda_1$, and channels (3) and (4) do so with a cutoff $\Lambda_2$. We make a three-dimensional plot by varying these two cutoffs and, again, the result is negative.

Generally speaking, the $B_s\pi$ and $B\overline{K}$ $S$-wave contributions calculated in Ref. [12] are around five times larger than any individual $P$-wave piece in the region of the $X(5568)$ resonance. When we replace $V(s)$ in Eq. (24) by $15\times V(s)$, we then find a pole at $5789 - i\,21$ MeV in the (1,1,1,0) sheet (which is in between the $B\overline{K}$ and $B^*\overline{K}$ mass thresholds) with a cutoff in the natural range, $\Lambda = 1$ GeV. This fact clearly indicates that the leading-order HMChPT $P$-wave potential that we have calculated is too weak to become resonant with a natural cutoff applied to the two-point unitarity loop functions. To a lesser extent this conclusion also holds for the $S$-wave case, as worked out in Ref. [12], whose results we also reproduce here. As for the dimensional regularization form of $G_i(s)$, cf. Eq. (21), the authors of Ref. [12] obtain $\alpha(\hat{\mu}) = -0.97 \pm 0.02$, with $\hat{\mu} = (m_{B_s^0} + m_{B^{*+}})/2 = 5323$ MeV. When translated to our scale this would correspond to $\alpha(M_\rho) \simeq -4.9$, which is clearly out of the range of natural values shown in Fig. 3. Indeed, we cannot generate such a value of $\alpha$ making use of Eq. (27) because the curvature would become dominant for higher mass thresholds and $\alpha$ does not become smaller than around $-4.3$. If we pursue along with the approximate linear behavior in Fig. 3, it would imply a mass threshold clearly larger than 7000 MeV, more than 1200 MeV higher than the $B\overline{K}$ threshold. However, if the isovector $B_s\pi - B\overline{K}$ $S$-wave potential is multiplied by a factor of 3 we then find a pole at $5548 - i\,23$ MeV with $\Lambda = 1$ GeV. This pole does not quantitatively agree with the experimental values for the mass and width of the $X(5568)$, but our point is to show that more strength in the potential is needed to generate the $X(5568)$ with natural cutoffs or natural values for the subtraction constants. We remark here that these exercises are just done for pure academic purposes, and that there is no physical reason to enhance the potential calculated by such factors. However, it helps us to understand better that if the observed $X(5568)$ is not found in the scattering amplitude evaluated with a natural cutoff is because the weakness of the leading-order HMChPT transition potentials, agreeing with the inference from Burns and Swanson [10]. These findings point to the direction that is hard to explain theoretically the experimentally reported $X(5568)$ by the D0 Collaboration. At least it cannot be described in a straightforward manner as a dynamically generated resonance by coupled-channel scattering, once the results of the $S$-wave study of Ref. [12] and the current $P$-wave attempt are taken simultaneously.

By an obvious replacement of the relevant masses, one can also explore the charm sector, namely, we have at hand the scattering of $D_s^+\pi^0$, $D_s^{*+}\pi^0$, $D^+\overline{K}^0$ and $D^{*+}\overline{K}^0$, with thresholds 2103.44, 2247.27, 2362.6 and 2499.97 MeV in order. No resonant pole for a partner state of the $X(5568)$ is found when a three-momentum cutoff around 1 GeV is used, in the lines of the criticism of Ref. [11].

## V. SUMMARY AND CONCLUSIONS

The recently observed exotic hadron candidate $X(5568)$ by the D0 Collaboration [1] in the $B_s^0\pi^\pm$ event distribution with quantum numbers $0^+/1^+$ has triggered interesting theoretical and experimental questions. In the present work, we first perform the analysis of the experimental event-distribution data by using a $P$-wave Breit-Wigner parameterization for the resonance signal function, instead of an $S$-wave BW as used by the D0 Collaboration in its analysis [1]. We fix the mass and width of the $P$-wave BW to the values obtained in Ref. [1] and the resulting fit reproduces data quite closely, being both fits (either assuming $S$- or $P$-wave $B_s^0\pi^\pm$) of similar quality.

We then make a complementary analysis by considering the $P$-wave coupled-channel scattering between the channels $B_s^0\pi^+$, $B_s^*\pi^+$, $B^+\overline{K}^0$ and $B^{*+}\overline{K}^0$. Notice that then $B_s\pi$ and $B_s^*\pi$ can couple each other and, indeed, the mass threshold for $B_s^*\pi$ is much closer to the nominal mass of the $X(5568)$ than the one for $B_s\pi$. This is an interesting point when one is considering the possible "molecular" nature for this resonance. It is clear that the $B_s\pi$ and $B_s^*\pi$ three-momenta are small (which presumably makes a $P$-wave scattering small), but the off-diagonal transitions involving the heavier $B\overline{K}$ and $B^*\overline{K}$

states have much larger *unphysical* three-momenta, determined by analytical continuation. The transition potential matrix $V(s)$ is calculated in leading-order Heavy Meson Chiral Perturbation Theory and it is then unitarized employing techniques of Unitary Chiral Perturbation Theory [13, 16, 31]. The subtraction constants appearing in the unitarization process are determined with almost coincident values, either by requiring the reproduction of the $B^{*0}$ simple pole in the $u$-channel $P$-wave scattering or by employing its natural values. We then search for poles in the resulting $T$-matrix and no pole that could be associated to the $X(5568)$ is found. The same conclusion is obtained when using the unitarity two-point loop functions calculated in terms of a three-momentum cutoff varied within a wide range around 1 GeV. If we further release the subtraction constants the $X(5568)$ pole could be imposed, but the resulting values for the subtraction constants prevent us from consider such a pole as dynamically generated from the $P$-wave interactions between the aforementioned two-body channels. In other terms, no explanation for its nature would then be obtained within our approach. Replacing the heavy $B$-like mesons by the corresponding charm ones, the charm sector can also be explored and similar results arise as well. We conclude that the main reason for the absence of poles is the weakness of the interactions.

In summary, by combining our $P$-wave study in the current work with the recent $S$-wave study of Ref. [12], the new state $X(5568)$ observed by D0 the Collaboration cannot be likely interpreted as a "molecular" resonance generated dynamically from two-body coupled-channel scattering. This point has also been supported by several other groups, see e.g. [6, 10, 11]. The nature of $X(5568)$ is still unsettled, and even its existence is inconclusive recalling also the experimental non-observation of this state by LHCb [9]. More theoretical and experimental efforts are still needed in order to settle these issues.

## ACKNOWLEDGEMENTS

We would like to thank E. Oset for a careful reading of the manuscript and interesting comments and X.W.K. would like to thank also M. Albaladejo for a clarification on the potential used in Ref. [12]. This work is supported in part by the MINECO (Spain) and ERDF (European Commission) grant FPA2013-40483-P and the Spanish Excellence Network on Hadronic Physics FIS2014-57026-REDT.

[1] V. M. Abazov *et al.* [D0 Collaboration], [arXiv:1602.07588 [hep-ex]].
[2] W. Wang and R. Zhu, arXiv:1602.08806 [hep-ph].
[3] W. Chen, H. X. Chen, X. Liu, T. G. Steele and S. L. Zhu, arXiv:1602.08916 [hep-ph].
[4] L. Tang and C. F. Qiao, arXiv:1603.04761 [hep-ph].
[5] Y. R. Liu, X. Liu and S. L. Zhu, Phys. Rev. D **93**, no. 7, 074023 (2016) [arXiv:1603.01131 [hep-ph]].
[6] S. S. Agaev, K. Azizi and H. Sundu, arXiv:1603.02708 [hep-ph]; S. S. Agaev, K. Azizi and H. Sundu, Phys. Rev. D **93**, no. 7, 074024 (2016) [arXiv:1602.08642 [hep-ph]].
[7] F. Stancu, arXiv:1603.03322 [hep-ph].
[8] Q. F. L and Y. B. Dong, arXiv:1603.06417 [hep-ph].
[9] The LHCb Collaboration, "Search for structure in the $B_s^0\pi^\pm$ invariant mass spectrum, LHCb-CONF-2016-004, available online `http://inspirehep.net/record/1430090/files/LHCb-CONF-2016-004.pdf`
[10] T. J. Burns and E. S. Swanson, arXiv:1603.04366 [hep-ph].
[11] F. K. Guo, U. G. Meißner and B. S. Zou, Commun. Theor. Phys. **65**, no. 5, 593 (2016) [arXiv:1603.06316 [hep-ph]].
[12] M. Albaladejo, J. Nieves, E. Oset, Z. F. Sun and X. Liu, Phys. Lett. B **757**, 515 (2016) [arXiv:1603.09230 [hep-ph]].
[13] J. A. Oller and E. Oset, Nucl. Phys. A **620**, 438 (1997) [Nucl. Phys. A **652**, 407 (1999)] [hep-ph/9702314].
[14] J. M. Alarcon, J. Martin Camalich, J. A. Oller and L. Alvarez-Ruso, Phys. Rev. C **83**, 055205 (2011); (E) *ibid.* **87**, 059901 (2013) [arXiv:1102.1537 [nucl-th]].
[15] J. M. Alarcon, J. Martin Camalich and J. A. Oller, Annals Phys. **336**, 413 (2013) [arXiv:1210.4450 [hep-ph]].
[16] J. A. Oller and U. G. Meißner, Phys. Lett. B **500**, 263 (2001) [hep-ph/0011146].
[17] D. Zieminska, for D0 collaboration, FNAL seminar on Feb. 25, 2016. `http://www-d0.fnal.gov/Run2Physics/WWW/results/final/B/B16A`
[18] K. A. Olive *et al.* [Particle Data Group Collaboration], Chin. Phys. C **38**, 090001 (2014).
[19] X. H. Liu and G. Li, arXiv:1603.00708 [hep-ph].
[20] M. B. Wise, Phys. Rev. D **45**, 2188 (1992).
[21] T. M. Yan, H. Y. Cheng, C. Y. Cheung, G. L. Lin, Y. C. Lin and H. L. Yu, Phys. Rev. D **46**, 1148 (1992) Erratum: [Phys. Rev. D **55**, 5851 (1997)].
[22] G. Burdman and J. F. Donoghue, Phys. Lett. B **280**, 287 (1992).
[23] J. M. Flynn *et al.* [RBC and UKQCD Collaborations], Phys. Rev. D **93**, no. 1, 014510 (2016) [arXiv:1506.06413 [hep-lat]].
[24] X. W. Kang, B. Kubis, C. Hanhart and U. G. Meiner, Phys. Rev. D **89**, 053015 (2014) [arXiv:1312.1193 [hep-ph]].
[25] Z. H. Guo and J. A. Oller, Phys. Rev. D **93**, no. 5, 054014 (2016) [arXiv:1601.00862 [hep-ph]].
[26] M. Jacob and G. C. Wick, Annals Phys. **7**, 404 (1959) [Annals Phys. **281**, 774 (2000)]; see applications in X. W. Kang et al., Phys. Lett. B **684**, 137 (2010) [arXiv:0912.3068 [hep-ph]]; Int. J. Mod. Phys. A **26**, 2523 (2011) [arXiv:1003.5494 [hep-ph]]; Phys. Rev. D **81**, 054032 (2010) [arXiv:0912.0899 [hep-ph]].
[27] E. Epelbaum, W. Glockle and U. G. Meißner, Nucl. Phys. A **747**, 362 (2005) [nucl-th/0405048]; R. Machleidt and D. R. Entem, Phys. Rept. **503**, 1 (2011) [arXiv:1105.2919 [nucl-th]].

[28] S. U. Chung, Phys. Rev. D **48**, 1225 (1993) Erratum: [Phys. Rev. D **56**, 4419 (1997)]; see applications in X. W. Kang et al., Chin. Phys. C **34**, 1061 (2010) [arXiv:0911.2998 [hep-ph]].
[29] A. Nogga, R. G. E. Timmermans and U. van Kolck, Phys. Rev. C **72**, 054006 (2005) [nucl-th/0506005].
[30] A. Lacour, J. A. Oller and U.-G. Meißner, Annals Phys. **326**, 241 (2011) [arXiv:0906.2349 [nucl-th]].
[31] J. A. Oller and E. Oset, Phys. Rev. D **60**, 074023 (1999) [hep-ph/9809337].
[32] J. A. Oller, Phys. Lett. B **477**, 187 (2000) [hep-ph/9908493].
[33] G. 't Hooft and M. J. G. Veltman, Nucl. Phys. B **153**, 365 (1979).
[34] J. A. Oller, Eur. Phys. J. A **28** (2006) 63 [hep-ph/0603134].
[35] D. Jido, E. Oset and A. Ramos, Phys. Rev. C **66**, 055203 (2002) [nucl-th/0208010].
[36] T. Becher and H. Leutwyler, JHEP **0106**, 017 (2001) [hep-ph/0103263].
[37] J. A. Oller, E. Oset and J. R. Pelaez, Phys. Rev. D **59**, 074001 (1999) Erratum: [Phys. Rev. D **60**, 099906 (1999)] Erratum: [Phys. Rev. D **75**, 099903 (2007)] [hep-ph/9804209].